

# MAGNETOSTATIC TORSIONAL ACTUATOR WITH EMBEDDED NICKEL STRUCTURES FOR PURE ROTATION

Tsung-Lin Tang<sup>1</sup>, Rongshun Chen<sup>1,2</sup>, and Weileun Fang<sup>1,2</sup>

<sup>1</sup>Power Mechanical Engineering, National Tsing Hua University, Hsinchu, Taiwan

<sup>2</sup>Institute of NanoEngineering and MicroSystems, National Tsing Hua University, Hsinchu, Taiwan

## ABSTRACT

This study demonstrates the magnetostatic torsional actuator consisting of a *Si-Ni* compound frame to significantly improve the driving force. The present design has three merits: (1) employ *Si* mold to simultaneously electroplate/pattern thick *Ni*, and the *Ni* and *Si* structures respectively provide magnetostatic force and superior mechanical properties, (2) the embedded *Ni* structures not only increase the ferromagnetic material volume but also enhance magnetization strength to enlarge magnetostatic torque, (3) the *Si-Ni* compound structure, which is nearly symmetric about the torsional axis, can decrease the moment of inertia and also reduce the wobble motion. Experiments show the *Si-Ni* compound scanner has optical scan angle  $\theta=90^\circ$ , and wobble motion and power consumption is significantly reduced.

## INTRODUCTION

Micro torsional actuators play an important role in various micro systems, such as micro scanner. The electrostatic and electromagnetic forces are two popular approaches to drive micro torsional actuator [1-4]. However, the pull-in effect and electrical isolation are two critical design considerations for electrostatic torsional actuators. The electromagnetic force has the advantage to drive torsional actuators with large displacement. Presently, Lorentz force [2-3] and magnetostatic force [4] are the most common electromagnetic driving forces for torsional actuators.

In general, for Lorentz force torsional actuator, the deposition of conducting film is required for the electrical routing of input current [2-3]. Moreover, the deposition of ferromagnetic film is required for magnetostatic force torsional actuator [4]. A thicker ferromagnetic (or conducting) film can increase the torque applied on torsional actuators. However, the film thickness is limited to the fabrication process. Moreover, the conducting and ferromagnetic films deposited on surface of *Si*-structures will introduce eccentric force and cause the unwanted wobble motion. The wobble motion of torsional actuator may lead problems for its applications, for instance, the reflective laser beam shake of micro scanner [5]. In order to suppress the unwanted wobble motion, the torsional actuator with axial symmetric structure design is required. Moreover, it is necessary to drive the actuator by pure torque. Thus, the complicated processes on double SOI (silicon-on-insulator) wafer [5] and the special torque generator design [6] have been reported.

This study presents the torsional actuator design consisting of *Si* substrate with embedded thick *Ni* structures

(*Si-Ni* compound). Thus, the volume of ferromagnetic material is significantly increase, and further increase the magnetostatic torque applying on the torsional actuator. Moreover, the wobble motion of the torsional actuator is reduced since the *Si-Ni* compound structure is nearly symmetric about the torsional axis. In applications, the optical scanners have been implemented to demonstrate the feasibility of the proposed design.

## CONCEPT AND DESIGN

This study employs the magnetostatic scanner in Fig.1 to demonstrate the proposed design concept. As indicated in Fig.1a, the scanner consisted of the torsional springs, *Si-Ni* compound frame, and mirror plate. The ferromagnetic *Ni* is patterned to slender shape and embedded in the *Si* frame. Fig.1a also shows the A-A' cross-section of the proposed design. The backside cavity provides a sufficient moving space for large scan angle operation. The proposed torsional actuator is driven by magnetostatic torque introduced by the *Si-Ni* compound frame. As illustrated in Fig.2, a magnetostatic torque  $T$  will apply on torsional actuator after

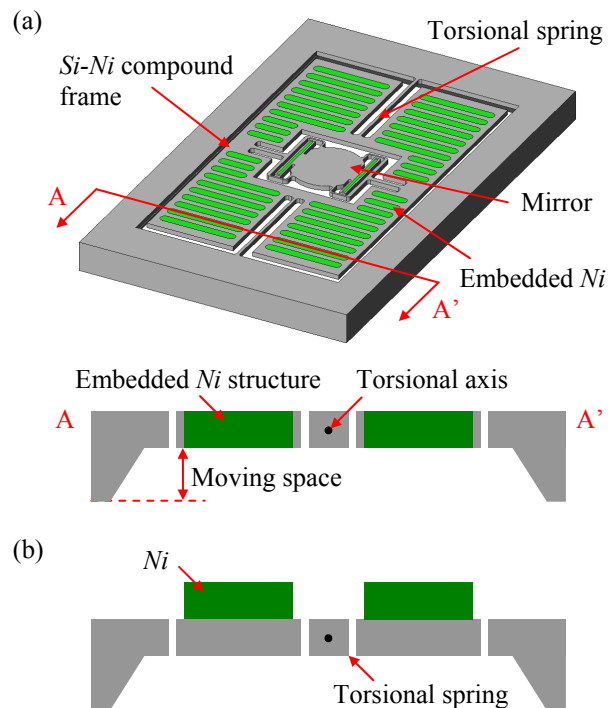


Figure 1: Design concepts, (a) top view of the torsional actuation device, and cross-section of *Ni* embedded inside *Si* structure, and (b) cross-section of existing design with *Ni* on *Si* surface.

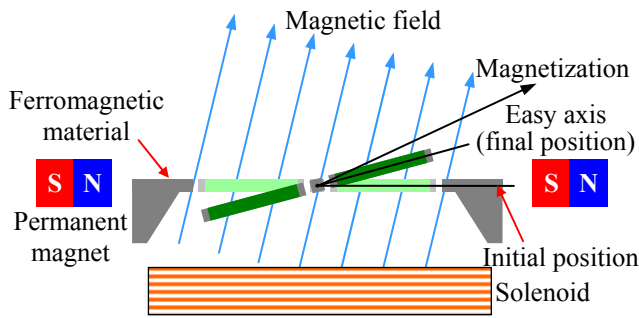




Figure 2: Actuation concepts of the scanner driven by magnetostatic force.

Table 1: Comparisons of Si-Ni compound structure and exiting design.

Design types	Items			Off-axis of CG (μm)	Resonant frequency (Hz)
	Ni	Si	Total		
Si-Ni compound structure 	5.81	1.90	7.71	0	690
Existing design 	5.84	3.42	9.26	50	630

introducing with a magnetic field  $H$ . The torque  $T$  is expressed as,

$$T = V_{mag} \cdot M \times H \quad (1)$$

where  $V_{mag}$  is the volume of ferromagnetic material embedded in the actuating frame,  $M$  is the magnetization. The permanent magnets near to the torsional actuator ensure the magnetization direction of ferromagnetic material. The magnetic field  $H$  is generated after applying current into the solenoid. From Eq.(1), the torque applying on the magnetostatic torsional actuator can be enlarged by increasing  $V_{mag}$  and  $M$ .

This study directly employs a patterned  $Si$  substrate as the mold to electroplate the ferromagnetic material. Thus, the thick ferromagnetic material can be electroplated and embedded into  $Si$  structure to increase  $V_{mag}$ . The ferromagnetic material is also patterned to slender shape to enhance magnetization  $M$ . In comparison, the ferromagnetic material in [4] is electroplated and patterned on the surface of  $Si$  structures, as in Fig.1b. Table 1 summarizes the characteristics of the proposed design and the one in Fig. 1b. As compare with the design in Fig. 1b, the proposed actuator can decrease the total moment of inertia to 83%. Moreover, the wobble motion induced by the off-axis of CG (center of gravity) is also reduced since the  $Si$ - $Ni$  compound actuating frame is nearly symmetric about the torsional axis.

## FABRICATION AND RESULTS

The magnetostatic torsional actuator was implemented by using the process shown in Fig.3. As in Fig.3a, the  $SiO_2$  was deposited and patterned at the backside of  $Si$  substrate to define the window for bulk  $Si$  etching. After that, the  $Si$  substrate was etched by  $TMAH$  to thin the structure thickness. As in Fig.3b, the  $Cr/Au/Ni$  layers were respectively deposited on the backside cavity of  $Si$  substrate as the adhesion-layer/seed-layer/supporting-layer. As in Fig.3c, the  $SiO_2$  hardmask at the front side of  $Si$  substrate was patterned, and then the  $DRIE$  process was used to define the  $Si$  structure. After removing the  $Cr$  adhesion-layer to expose the  $Au$  seed-layer, the embedded  $Ni$  structure was electroplated and molded. As in Fig.3d, after stripping the  $Ni$  supporting-layer and  $Au$  seed-layer from back side, the  $SiO_2$  hardmask was patterned and the  $DRIE$  was used to define the  $Si$  structure. Finally, the  $Cr$  adhesion-layer and  $SiO_2$  were removed to release the device, as shown in Fig.3e.

More detail regarding the implementation of the embedded  $Ni$  structure is shown in Fig.4. As indicated in Fig.4a, the  $Si$  mold for  $Ni$  electroplating was defined by  $DRIE$  and the  $Cr$  adhesion-layer was patterned by wet etching. The  $Au$  seed-layer was only  $0.2\mu m$  thick. Hence, the suspended thin  $Au$  seed-layer would easily be damaged during the following fabrication processes. In this regard, the  $Ni$  supporting-layer ( $15\mu m$ ) was employed to support and protect the thin seed-layer. After the electroplating process in Fig.4b, the bulk  $Ni$  material was embedded in the  $Si$  structure. This method can avoid the problems induced by the non-uniformity of seed-layer deposited on  $Si$  mold [8].

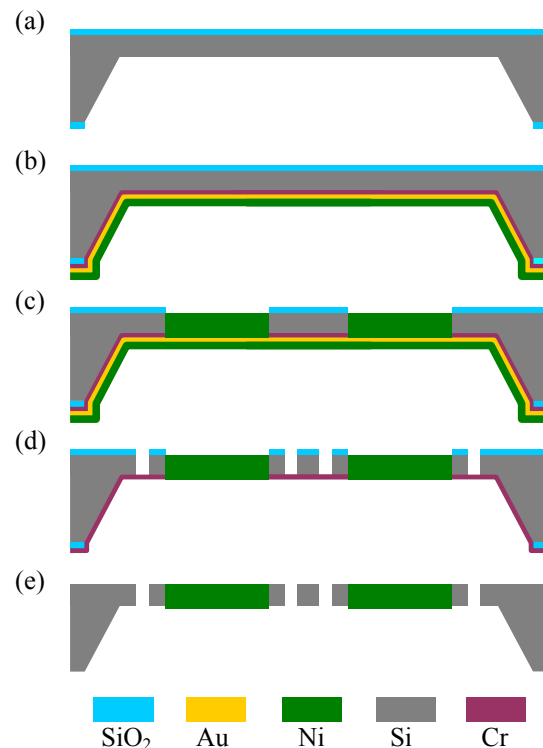


Figure 3: Fabrication process flow.

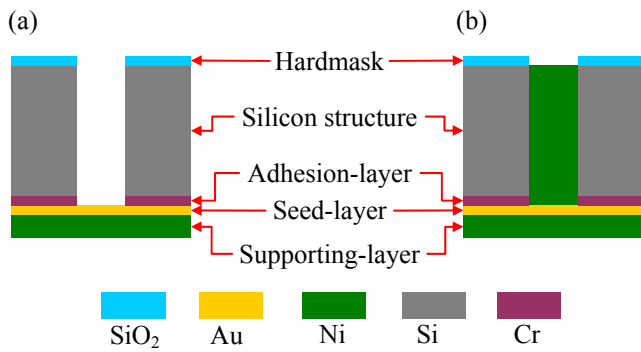


Figure 4: Implementation of the embedded Ni structure, (a) before and (b) after embedding the bulk Ni.

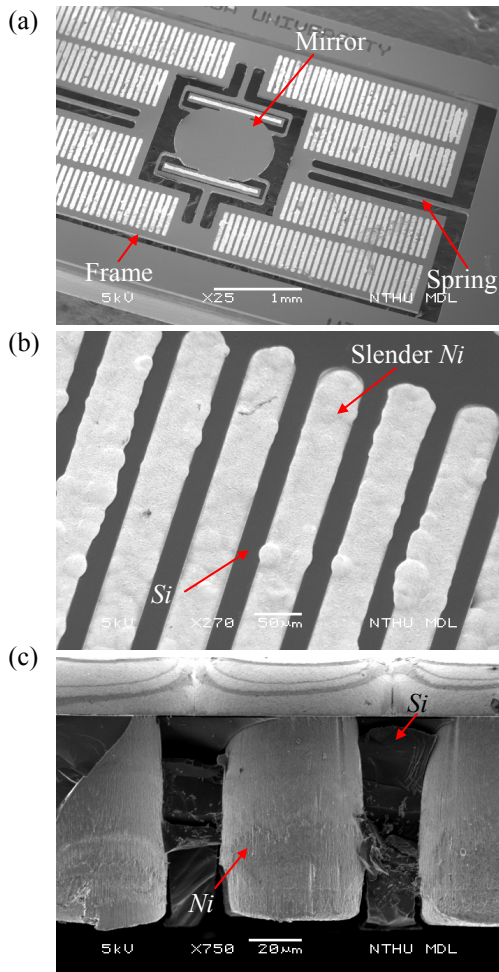


Figure 5: SEM micrographs of (a) front-side of a typical fabricated scanner, (b) Si-Ni compound actuating frame, and (c) cross-section of embedded Ni structures.

The SEM micrograph in Fig.5a shows the front-side of a typical fabricated torsional actuator. The mirror, Si-Ni compound frame, and torsional springs are observed. The frame is embedded with the slender Ni structures to increase the magnetostatic torque. The zoom-in micrographs in Fig.5b-c show the top-view and cross-section of Ni-Si compound structures. It is clearly observed the

electroplating Ni was successfully molded and patterned by the Si structures. The Si frame and the embedded Ni structure are near  $80\mu\text{m}$  thick, and the aspect ratio of the presented Ni structure is 2.

## EXPERIMENTS AND DISCUSSIONS

In applications, a micro scanner driven by the presented magnetostatic torsional actuator is demonstrated. As in Fig.6a, a  $5\text{mm}\times 8\text{mm}$  chip containing the micro scanner, the permanent magnets, and the solenoid are assembled on a stage. The permanent magnets are employed to specify a magnetic field to ensure the magnetization direction of the embedded Ni structures. The solenoid embedded in the stage provides a periodic magnetic field to actuate the scanner. Fig.6b shows the driving test of the scanner in a scan angle measurement stage. For typical test results, the scanner was operated at  $593\text{Hz}$  with optical scan angle  $\theta = 90^\circ$  using  $81\text{mW}$  input power. In comparison, the scanner in [4] is operated at  $367\text{Hz}$  with  $\theta = 88^\circ$  using  $170\text{mW}$  input power. Therefore, the magnetostatic scanner has better operation performance.

Fig.7 shows measurements of out-of-plane wobble motion on torsional spring by Laser Doppler Vibrometer. As limited by the numerical aperture of objectives, the measurements are only available for small scan angles. While scanning at  $\theta = 3^\circ$ , the wobble displacements of existing design [7] is  $56\text{nm}$ , and the proposed design is only  $20\text{nm}$ . Note the excitation frequency by the periodic eccentric force is double the scanning frequency. The frequency of wobble motion is double the scanning frequency. Thus, the out-of-plane wobble motion is significantly reduced by the proposed design.

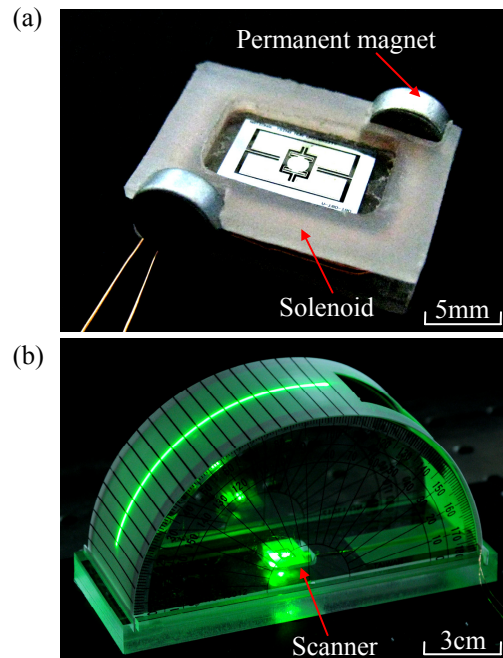


Figure 6: Experiment setup, (a) driving stage, and (b) measurement of the optical scan angle.

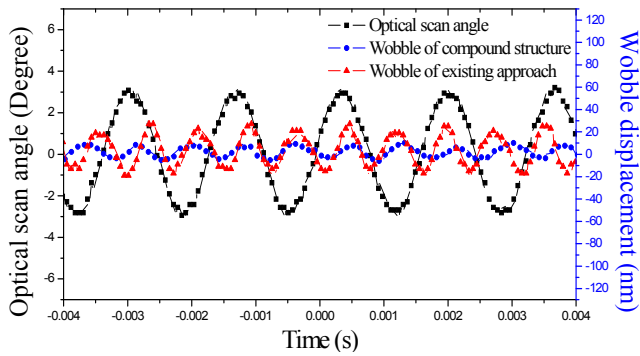


Figure 7: Displacements of out-of-plane wobble motion.

## CONCLUSION

This study presents a magnetostatic torsional actuator design consisting of a novel *Si-Ni* compound frame. This study also establishes the process to apply the *Si* substrate as a mold for *Ni* electroplating to implement the torsional actuator with *Si-Ni* compound frame. The *Si-Ni* compound frame with thick and slender *Ni* structures is designed to increase the volume and magnetization of the ferromagnetic material. Thus, the driving torque for the magnetostatic torsional actuator is significantly improved. Since the *Si-Ni* compound frame is nearly symmetric about the torsional axis, the proposed design is also reduce the wobble motion. The measurement results show that the proposed design has the optical scan angle of  $90^\circ$ . In comparison, the input power has been decreased for 2-fold (from 170mW to 81mW), and the out-of-plane wobble motion is reduced for 3-fold (from 56nm to 20nm).

## ACKNOWLEDGEMENTS

This paper is based (in part) upon work supported by the National Science Council, Taiwan under Grant NSC 96-2628-E-007-008-MY3. The authors would like to express his appreciation to the Nano Science and Technology Center of National Tsing Hua University, and Nano Facility Center of National Chiao Tung University in providing the fabrication facilities.

## REFERENCES

- [1] S. Hsu, T. Klose, C. Drabe, and H. Schenk, "Fabrication and Characterization of A Dynamically Flat High Resolution Micro-Scanner", *Journal of Optics A*, vol. 10, pp. 044005, 2008.
- [2] J. Tauscher, W. O. Davis, D. Brown, M. Ellis, Y. Ma, M. E. Sherwood, D. Bowman, M. P. Helsel, S. Lee, and J. W. Coy, "Evolution of MEMS Scanning Mirrors for Laser Projection in Compact Consumer Electronics", *Proc. of SPIE*, vol. 7594, pp. 75940A, 2010.
- [3] A. D. Yalcinkaya, H. Urey, D. Brown, T. Montague, and R. Sprague, "Two-Axis Electromagnetic Microscanner for High Resolution Displays", *Journal of Microelectromechanical Systems*, vol. 15, pp.786-794, 2006.
- [4] A. D. Yalcinkaya, H. Urey, and S. Holmstrom, "NiFe Plated Biaxial MEMS Scanner for 2-D Imaging", *IEEE Photonics Technology Letters*, vol. 19, pp. 330-332, 2007.
- [5] Y. Mizoguchi and M. Esashi, "Design and Fabrication of A Pure-Rotation Microscanner with Self-Aligned Electrostatic Vertical Comdrives in Double SOI Wafer", in *Digest Tech. Papers Transducers'05 conference*, Seoul, June 5-9, 2005, pp.65-86.
- [6] H.-Y. Lin and W. Fang, "A Rib-Reinforced Micro Torsional Mirror Driven by Electrostatic Torque Generators", *Sensors and Actuators A*, vol. 105, pp.1-9, 2003.
- [7] T.-L. Tang, C.-P. Shu, W.-C. Chen, and W. Fang, "Design and Implementation of A Torque-Enhancement 2-Axis Magnetostatic SOI Optical Scanner", *Journal of Micromechanics and Microengineering*, vol. 20, pp. 025020, 2010.
- [8] D. Malta, C. Gregory, D. Temple, C. Wang, T. Richardson, and Y. Zhang, "Optimization of Chemistry and Process Parameters for Void-Free Copper Electroplating of High Aspect Ratio Through-Silicon Vias for 3D Integration", *Electronic Components and Technology Conference*, San Diego, May 26-29, 2009, pp.1301-1306.